Proceedings of the 21st ICSMGE, Vienna, Austria, 14 – 19 June 2026. Pistrol, Adam & Schweiger (eds.)
Published by: ÖGG, Austrian Society for Geomechanics, Salzburg, Austria, ISBN 978-3-9503898-4-5
https://doi.org/10.53243/ICSMGE2026-1805

Finite element modeling of piping erosion process based on hole erosion test results

Dalia Ayssami, Sahar Hemmati, Yasmina boussafir, Christophe Chevalier, Philippe Reiffsteck
Université Gustave Eiffel, GERS-SRO, F-77454 Marne-la-Vallée, France

ABSTRACT: Internal erosion is a critical failure mechanism in levees and earth dams, where water flow gradually removes soil particles, potentially leading to progressive damage. Among its various forms, piping erosion is particularly dangerous, as it begins at the downstream side and advances upstream, often resulting in sudden structural collapse. While experimental techniques such as the Hole Erosion Test (HET) provide essential parameters like critical shear stress and erosion rate, they do not fully capture the complex interactions between flow dynamics, sediment transport, and cavity evolution. This study presents a numerical model in order to simulate the localized enlargement of a hole within cohesive soil subjected to hydraulic loading due to water flow. Implemented in COMSOL Multiphysics®, the model couples turbulent fluid flow, modeled with the Reynolds-Averaged Navier-Stokes equations and a standard k-ε turbulence model, sediment transport, governed by an advection-dispersion equation, and geometry evolution using an erosion law. The geometry is updated dynamically using the Arbitrary Lagrangian-Eulerian (ALE) method, enabling the simulation of continuous cavity enlargement. The model is validated using experimental HET measurements. Simulation results accurately reproduce key observed phenomena, including the increase in flow rate, the concentration of eroded particles at the outlet, and the progressive enlargement of the hole. The influence of critical shear stress and erosion coefficient is clearly reflected in the model's predictions, which align closely with laboratory results.
This approach provides a physically based tool to study internal erosion under realistic flow conditions. It represents a step toward more advanced simulations capable of addressing complex geometries, anisotropic soils, and full-scale backward erosion scenarios.

KEYWORDS: Internal erosion, Hole erosion test (HET), Sediment transport, Advection-dispersion, Cavity evolution, Numerical modeling, Soil–water interaction

1 INTRODUCTION

The erosion is the most important failure mechanism for dams and levees, (Fry et al., 2015). Modeling the internal erosion process poses a major challenge due to its very slow kinetics at the field scale, often unfolding over several decades. Laboratory experiments attempt to accelerate erosion by applying high hydraulic gradients. As a result, laboratory tests and numerical modeling have become complementary approach for investigating the hydro-mechanical behavior of erodible soil.

Initial models based on porous media theory, such as that proposed by (Vardoulakis et al., 1996), treat soil as a multiphase system and simulate erosion using mass balance and fluid flow equations. This foundational work was later extended by (Papamichos and Vardoulakis, 2005) to incorporate mechanical degradation linked to increasing porosity. Other researchers (Cividini et al., 2009; Uzuoka et al., 2012; Zhang et al., 2019) have further developed these approaches, although most still simplify the mechanical response.

Recent models have turned attention to suffusion and fine particle migration (Deng et al., 2023), channel evolution under hydrodynamic stress (Kahza and Sanaei, 2024), and hole erosion in cohesive soils (Mercier et al., 2015). These researches improve erosion tracking but often require experimental validation.

Advanced numerical frameworks have also been developed, such as those by (Nieber et al., 2019) using COMSOL with turbulent flow models; and by Rotunno et al. (2019) and Robbins et al. (2021), who modeled regressive erosion while accounting for spatial variability in soil properties. Collectively, these studies demonstrate the growing sophistication and importance of numerical modeling in capturing internal erosion processes that are difficult to observe directly.

2 NUMERICAL MODEL

A 2D axisymmetric numerical model of the Hole Erosion Test (HET) is presented, developed using COMSOL Multiphysics. The flow through the central hole is simulated with the CFD module, while the transport of detached particles is modeled via an advection-dispersion equation using the Coefficient Form PDE module. The Deformed Geometry interface is employed to update the domain as the hole enlarges due to erosion. The objective is to assess the model ability to replicate experimental observations.

2.1 *Governing equations*

Water flow in the hole is governed by the Reynolds-Averaged Navier–Stokes (RANS) equations, which account for turbulence effects:

$$\rho_w(\nabla.\boldsymbol{U}) = 0 \tag{1}$$

$$\rho_w \frac{\partial \boldsymbol{U}}{\partial t} + \rho_w(\mathbf{U}.\nabla)\boldsymbol{U} = \nabla.\mathbf{F} \tag{2}$$

$$\boldsymbol{F} = -p\boldsymbol{I} + 2\mu_w\boldsymbol{S} + \boldsymbol{K} \tag{3}$$

$$\boldsymbol{S} = \frac{1}{2}[\nabla\boldsymbol{U} + (\nabla\boldsymbol{U})^T] \tag{4}$$

where, U is the velocity vector ($m.s^{-1}$), p is the static pressure (Pa), μ_w is the dynamic viscosity of water (Pa.s), S is the symmetric part of the velocity, I is the second-order identity tensor and K is the turbulent stress tensor representing momentum transfer due to velocity fluctuations.

To model the evolution of suspended particle concentration downstream of the hole, COMSOL Multiphysics Coefficient Form PDE interface is used, enabling implementation of the advection-dispersion equation in an axisymmetric domain. This classic equation in sediment transport modeling is expressed as:

$$\frac{\partial co}{\partial t} + \nabla.(-c\nabla co) + \beta.\nabla co = 0 \quad (5)$$

where co is the concentration of suspended sediments (kg.m^{-3}), c is turbulent dispersion coefficient (m^2.s^{-1}), $\beta = (0, u)$ and u is the water flow velocity.

The progressive enlargement of the hole is modeled in COMSOL using the Deformed Geometry interface, which allows for dynamic updates to vary the shape of the computational domain based on the evolution of the simulated physical processes. In our case, the boundary between the hole and the soil, representing the internal wall of the eroded hole, is defined as a moving interface, allowed to displace only in the radial direction (r), and uniformly along its entire length.

2.2 *Geometry and mesh*

To reduce calculation time, a 2D axisymmetric model, presented in Figure 1 is used instead of a full 3D simulation. The geometry includes a central hole (3 mm in diameter) and an adjacent erodible soil zone, both modeled as rectangles. The domain is discretized with a quadrilateral mesh using quadratic interpolation. A very fine mesh (max 0.35 mm) is applied near the hole to capture detailed flow and erosion effects. A coarser, depth-increasing mesh is used in the surrounding soil. Several mesh refinement tests were performed in order to ensure stable, efficient coupling of flow, particle transport, and geometry deformation.

2.3 *Boundary conditions*

Turbulent water flow is applied exclusively in Zone B, the hole (Figure 1), using the k–ε model. Regarding boundary conditions:

On boundary 1, a constant hydrostatic pressure set to the value measured during the test for flow equation, and advection condition are applied for concentration equation. On boundary 3, located at the outlet of the hole a zero hydrostatic pressure is imposed, assuming negligible pressure at the outlet compared to the upstream and also a zero concentration.

Boundary 2, which represents the wall between the hole and the soil, is modeled as a No-Slip Wall with roughness. This approach approximates the head losses observed in the system and aligns simulated discharge rates with experimental measurements. A source condition $\dot{\varepsilon}$ (kg.m^{-2}.s^{-1}) is used to model sediment input from erosion on boundary 2, and calculated according to the erosion law, defined by the following:

$$\dot{\varepsilon} = k_{er}(\tau - \tau_{cr}) \quad (6)$$

Where, k_{er} is the erosion coefficient (s.m^{-1}), τ: is the shear stress (often used in fluid dynamics or geomechanics), τ_{cr} is the critical shear stress (Pa). These parameters are measured from Hole Erosion Test (Afnor, 2024, XP P94-065).

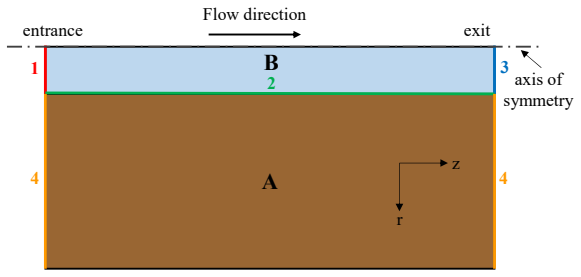

Figure 1. Model geometry and boundaries

On the inner boundary of the hole (boundary 2), a Prescribed Normal Mesh Velocity condition was applied. This boundary represents the eroded wall of the hole, whose displacement is directly governed by the erosion velocity. The latter is calculated using the erosion law previously introduced and expressed here as:

$$\frac{\partial r_t}{\partial t} = \frac{k_{er}(\tau - \tau_{cr})}{\rho_s} \quad (7)$$

where r_t is the hole radius, and ρ_s is the solid grains density (kg.m^{-3}).

This formulation directly links the mesh displacement velocity to the intensity of the erosion process, thereby ensuring a geometric evolution that is consistent with the physical phenomenon being modeled.

3 RESULTS AND DISCUSSIONS

In this section, the main results obtained from the numerical simulations are presented.

The simulations were conducted under transient conditions; "time-dependent" calculations, simulated over a period corresponding to the associated experimental test. The results shown in Figure 2 illustrate the evolution of particle concentration in suspension within the eroded hole. Each time step is accompanied by two zoomed-in frames at the inlet and outlet of the hole, in order to better visualize the details in these key zones. These profiles are used to illustrate the progressive accumulation of particles within the conduit, in relation to the passage of time and the widening of the hole.

At the beginning of the test (Figure 2.a), the concentration is observed to remain very low across the entire domain, with a slight appearance of particles mainly at the outlet. This distribution is directly governed by the flow direction, with the first detached particles being transported downstream. The upstream zone remains nearly empty, indicating that no significant accumulation is formed at the hole's entrance. At this stage, the concentration field is still localized, with only small colored regions being detected. As the test progresses (Figure 2.b-c), the concentration is seen to increase significantly, spreading over a growing portion of the hole, while maintaining a marked gradient from upstream to downstream. The downstream area becomes noticeably more loaded with particles, while the upstream region remains relatively sparse. This asymmetry is explained by the preferential transport induced by the flow, with particles being continuously carried toward the outlet. In the zoomed-in areas, this trend can clearly be observed: concentration contours are shown to be much more intense and widespread at the outlet than at the inlet.

Simultaneously, the zoomed views allow the progressive enlargement of the hole over time to be clearly observed. The inner wall of the conduit is gradually displaced outward, reflecting the continuous erosion of material along the periphery of the hole. This displacement is governed by the erosion law implemented in the model, which determines the rate of enlargement based on local hydraulic stresses. The geometric evolution is made possible by the "Deformed Geometry" interface, through which the boundary between intact soil and the eroded cavity is dynamically updated, exclusively in the radial direction.

By the end of the simulation (Figure 2.d), a marked concentration of particles is observed at the outlet, with high-intensity zones extending across the entire height of the conduit. The upstream region, on the other hand, remains much less

concentrated, confirming the dominant role of advection in particle transport. The evolution of the concentration fields, together with the visible enlargement of the conduit in the zoomed-in frames, demonstrates that the model is capable of faithfully reproducing the dynamics of a flow localized within a widening hole.

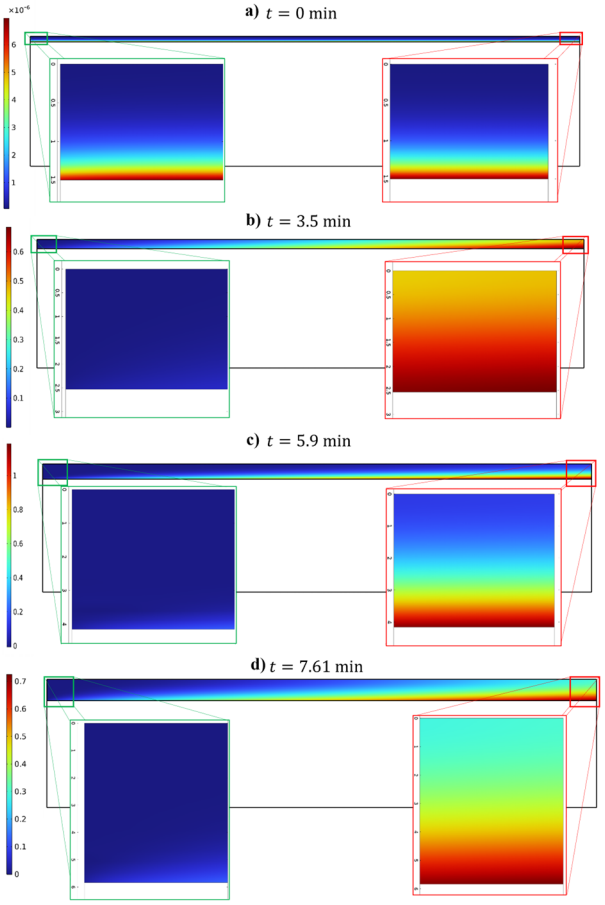

Figure 2. Evolution of suspended particle concentration (kg.m^{-3}) and hole widening over time

Figure 3.a shows the evolution of the radial velocity of the inner wall of the hole, which locally reflects the intensity of the enlargement process. Overall, the temporal trend is well captured by the model for the test: a gradual acceleration over time, with final values close to those measured. The numerical results correctly follow the general trend, although naturally smoothed, whereas the experimental data show more irregular variations. These peaks and troughs observed in the experimental results are likely linked to local soil instabilities or irregularities in the shape of the hole, which the smoothed model cannot reproduce.

Figure 3.b compares the concentration of solid particles at the outlet of the hole. The numerical results reproduce the orders of magnitude and general trends observed, showing a gradual increase in concentration over time. However, the experimental curve shows more frequent and sometimes abrupt fluctuations, which may result from localized detachment mechanisms or sudden arrivals of particles released from the erosion front. These irregular phenomena, typical of non-homogeneous granular media, are difficult to predict in a continuous model. The model, based on averaged formulations and time-smoothed conditions, yields a more regular response, making some of the experimentally observed fluctuations less apparent. This difference does not undermine the overall relevance of the modeling, which correctly reflects the cumulative evolution of the phenomenon.

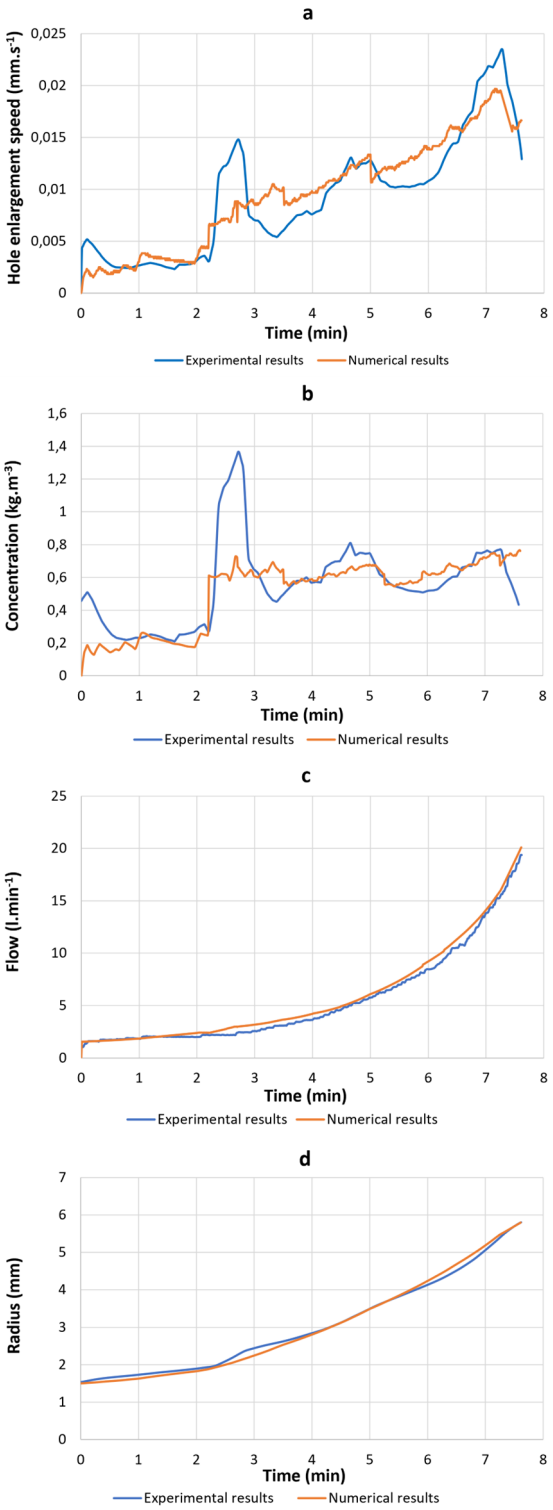

Figure 3. Comparison between numerical results (orange) and experimental results (blue) based on the evolution of four parameters: hole propagation speed, outlet concentration, inlet flow rate, and hole radius.

The flow rate at the hole inlet is presented in Figure 3.c. The agreement is remarkably good between measurements and calculations. The numerical and experimental curves follow the same increasing trend, with very small deviations throughout the tests. This good match confirms the relevance of the hydraulic parameter calibration, particularly the treatment of head losses through the equivalent roughness, as well as the model ability to predict the evolution of the flow in an enlarging hole.

Finally, the Figure 3.d, which represents the evolution of the hole radius, highlights a very good level of agreement between measurements and numerical predictions. The curves are nearly superimposed, even during the accelerated growth phases of the hole. This indicates that the implemented erosion law, combined with the boundary displacement strategy via the Deformed Geometry interface, enables consistent simulation of the conduit enlargement kinematics, without notable drift over the duration of the test.

Overall, this comparison between numerical and experimental data validates the model's ability to accurately reproduce the main evolutionary trends of the four key quantities. While some local discrepancies remain in the more sensitive signals - such as concentration or enlargement velocity - they remain within an acceptable range, considering the intrinsic complexity of the phenomena studied and the averaged nature of the equations used.

4 CONCLUSIONS

This study presented a numerical approach for modeling internal erosion processes, focusing on the enlargement of a hole within a porous medium. Using COMSOL Multiphysics, a 2D axisymmetric model was developed and successfully validated using experimental Hole Erosion Test (HET) results.

The model effectively captured the temporal evolution of key physical variables, including wall displacement, flow velocity, particle concentration, and hole radius. The numerical results closely matched experimental observations, confirming the reliability of the erosion law and the calibrated hydraulic parameters.

The use of a dynamic "Deformed Geometry" interface enabled consistent simulation of geometry evolution, while the coupling of turbulent flow and particle transport equations allowed for a detailed representation of flow-erosion interactions. Notably, the model reproduced the concentration gradients observed in experiments, reflecting the dominant advective transport.

Although some local discrepancies persisted, mainly in concentration fluctuations and timing, these remained within acceptable bounds, given the complexity of the physical processes and the model continuous formulation.

This validated framework provides a solid foundation for extending the model to incorporate regressive erosion propagation and stochastic effects related to soil heterogeneity. As such, it offers a valuable predictive tool for understanding erosion-driven failures in geotechnical structures.

5 ACKNOWLEDGEMENTS

This work was supported by Université Gustave Eiffel and the French General Directorate for Risk Prevention (DGPR). The authors would like to express their sincere gratitude for the financial and institutional support provided, which made this research possible.

6 REFERENCES

Afnor, 2024. Sols: reconnaissance et essais - Hole Erosion Test - Principe et méthode d'essai en laboratoire pour la détermination des caractéristiques de résistance à l'érosion de conduit. XP P94-065

Cividini, A., Bonomi, S., Vignati, G.C. and Gioda, G., 2009. Seepage-Induced Erosion in Granular Soil and Consequent Settlements. *International Journal of Geomechanics*, 9(4), pp.187–194. https://doi.org/10.1061/(ASCE)1532-3641(2009)9:4(187).

Deng, Z., Wang, G., Jin, W., Tang, N., Ren, H. and Chen, X., 2023. Characteristics and quantification of fine particle loss in internally unstable sandy gravels induced by seepage flow. *Engineering Geology*, 321, p.107150. https://doi.org/10.1016/j.enggeo.2023.107150.

Fry, J.J., François, D., Marot, D., Bonelli, S., Royet, P., Chevalier, C. and Deroo, L., 2015. Etude de l'érosion interne: apport du projet Eniroh. 25ème congrès des Grands Barrages. Stavanger, Norvège. pp.486–507.

Kahza, H.E. and Sanaei, P., 2024. Mathematical modeling of erosion and deposition in porous media. *Physical Review Fluids*, 9(2), p.024301. https://doi.org/10.1103/PhysRevFluids.9.024301.

Mercier, F., Bonelli, S., Golay, F., Anselmet, F., Philippe, P. and Borghi, R., 2015. Numerical modelling of concentrated leak erosion during Hole Erosion Tests. *Acta Geotechnica*, 10(3), pp.319–332. https://doi.org/10.1007/s11440-014-0349-5.

Nieber, J.L., Wilson, G.V. and Fox, G.A., 2019. Modeling Internal Erosion Processes in Soil Pipes: Capturing Geometry Dynamics. *Vadose Zone Journal*, 18(1), pp.1–13. https://doi.org/10.2136/vzj2018.09.0175.

Papamichos, E. and Vardoulakis, I., 2005. Sand erosion with a porosity diffusion law. *Computers and Geotechnics*, 32(1), pp.47–58. https://doi.org/10.1016/j.compgeo.2004.11.005.

Robbins, B.A., Griffiths, D.V. and Fenton, G.A., 2021. Random finite element analysis of backward erosion piping. *Computers and Geotechnics*, 138, p.104322. https://doi.org/10.1016/j.compgeo.2021.104322.

Rotunno, A.F., Callari, C. and Froiio, F., 2019. A finite element method for localized erosion in porous media with applications to backward piping in levees. *International Journal for Numerical and Analytical Methods in Geomechanics*, 43(1), pp.293–316. https://doi.org/10.1002/nag.2864.

Uzuoka, R., Ichiyama, T., Mori, T. and Kazama, M., 2012. Hydro-mechanical analysis of internal erosion with mass exchange between solid and water. 6th International Conference on Scour and Erosion. Paris.

Vardoulakis, I., Stavropoulou, M. and Papanastasiou, P., 1996. Hydro-mechanical aspects of the sand production problem. *Transport in Porous Media*, 22(2), pp.225–244. https://doi.org/10.1007/BF01143517.

Zhang, L., Wu, F., Zhang, H., Zhang, L. and Zhang, J., 2019. Influences of internal erosion on infiltration and slope stability. *Bulletin of Engineering Geology and the Environment*, 78(3), pp.1815–1827. https://doi.org/10.1007/s10064-017-1185-2.

COMSOL Multiphysics® v. 6.3. www.comsol.com.